Control of Hybrid Electric Vehicles

ANTONIO SCIARRETTA and LINO GUZZELLA

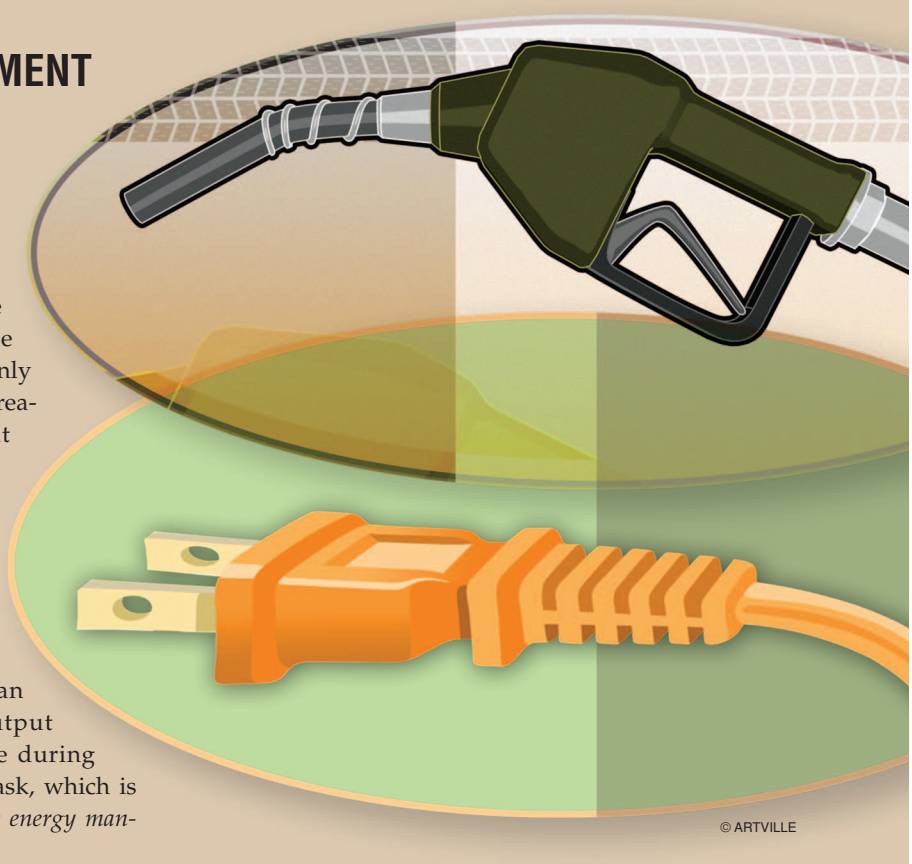

OPTIMAL ENERGY-MANAGEMENT STRATEGIES

Although hybrid electric vehicles (HEVs) have existed since before 1900 (Figure 1), interest in these vehicles has grown substantially only in the last 15–20 years. The main reason for this interest is the expectation that HEVs represent a short-term approach to improving fuel efficiency and reducing pollutant emissions of automobiles. In internal-combustion-engine (ICE) systems, the mechanical power needed to drive the vehicle is provided by the engine, whereas in HEVs, an engine and additional energy source (usually, an electric motor fed by an electrochemical battery) combine their output power. How the power split is to be made during vehicle operation comprises a new control task, which is often referred to as the *supervisory control* or *energy management* problem.

Compared to conventional ICE systems, a hybrid propulsion system can save fuel for the following reasons: an HEV can recover part of the vehicle's kinetic energy while braking and use this energy at a later time; an HEV can shut down the ICE during idling and low-load phases without compromising the driveability of the vehicle due to the high bandwidth of the electrically generated torque; an HEV can avoid low-efficiency operating points of the ICE by first storing excess power in the batteries and later driving the vehicle in an electric-only mode; and, since the electric motor can provide some of the torque during short acceleration phases, the ICE in an HEV can be designed with a smaller displacement and, thus, a better average efficiency.

The achievable improvement in fuel economy depends strongly on the vehicle and the driving cycle; realistic figures range from below 10% for mild hybrids to more than 30% for highly hybridized vehicles. This potential can be realized only with a sophisticated control system that optimizes energy flow within the vehicle. This observation has spurred a considerable amount of research in the last 15 years, as evidenced by the data shown in Figure 2, representing the number of papers published by IEEE from 1990 to 2004 containing the keywords "hybrid vehicle."

Early energy-management controllers were based on heuristic considerations inspired by the expected behavior of the propulsion system. For instance, the maximum torque of an ICE is low at low speeds, while electric motors can usually produce high low-speed torques. Thus, a common control strategy is to run the powertrain in a purely electrical mode from standstill to a chosen vehicle speed. At this speed the electric motor reaches its torque limit, and the engine is turned on. Similar control rules have been derived using heuristic approaches, with the resulting strategies formalized as Boolean or fuzzy rules [2].

1066-033X/07/$25.00©2007IEEE

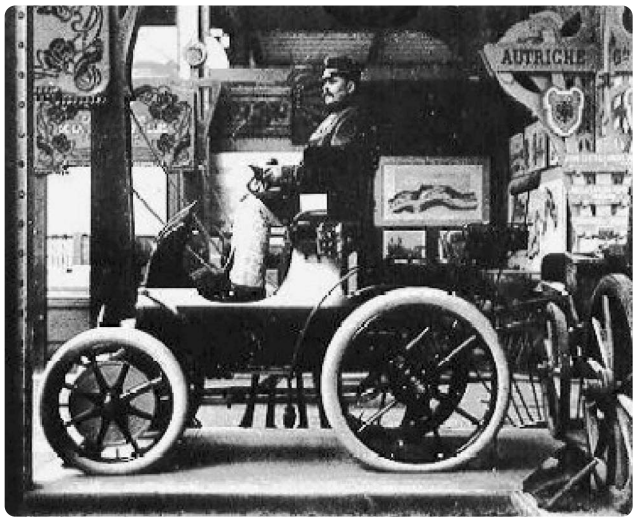

FIGURE 1 Ferdinand Porsche's first hybrid vehicle, produced by the Austrian company Jacob Lohner & Co. (1899). The powertrain was a series hybrid, with an engine-generator providing the electricity to drive four wheel-mounted electric motors [1].

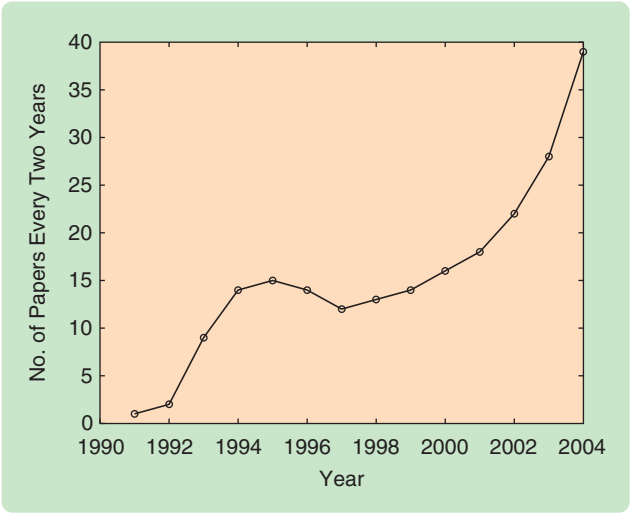

FIGURE 2 Research trend in the control of hybrid vehicles. The curve shows the number of papers in the IEEE database containing the key words "hybrid vehicle."

the various parameters, such as the speed threshold at which the ICE is started, depend strongly on the particular HEV system as well as on the driving conditions. Thus, a costly experimental calibration activity is usually necessary. Moreover, control parameters that perform well under certain conditions may lead to poor behavior under different conditions.

One way to resolve these difficulties is to adopt systematic, model-based optimization methods using meaningful objective functions. These methods can improve the system structure, its parameters, or the energy-management controller. In this article we focus on the last objective, assuming that the HEV structure and components are fixed. Serial, parallel, and combined HEV structures are defined and discussed in the next section. We then provide a meaningful definition of optimal behavior of an HEV, followed by an illustration of the use of optimization techniques. Finally, we describe how optimal controllers can be implemented in real time.

HEV ARCHITECTURES AND ENERGY MANAGEMENT

The energy-flow diagram of a combined HEV powertrain is shown in Figure 3. This HEV structure is a general powertrain architecture. Simpler architectures can be derived by omitting some of the paths and nodes. A parallel HEV structure is obtained by deleting paths P_N and P_G. A series HEV structure does not contain the path P_C or the gear and clutch block. Practical implementation of the combined HEV concept may require that some nodes or paths be physically linked. For example, the Toyota Prius structure [3], which constitutes a power-split architecture, includes a planetary gear set that corresponds to the dashed block of Figure 3.

Serial HEV structures are advantageous with respect to pollutant emissions, but have serious disadvantages with respect to fuel economy. Parallel and combined HEV structures can achieve both excellent fuel economy and very low pollutant emissions. Therefore, we focus on these HEV structures and only briefly discuss series HEV structures.

The number of degrees of freedom (DOFs) in the energy flow of a hybrid powertrain is related to the number of

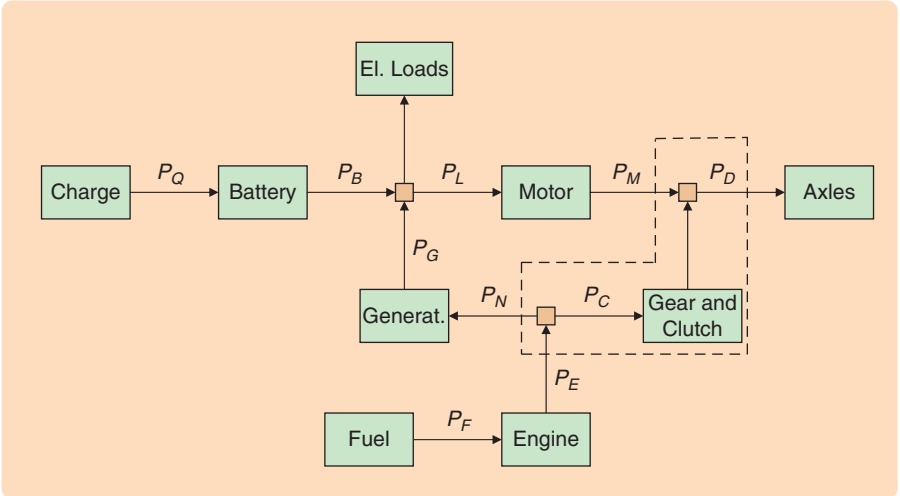

FIGURE 3 Energy flow of a general hybrid powertrain. The dashed block can be physically realized with a planetary gear set.

nodes in its energy-flow diagram. Ignoring the DOF allowed by variable transmission ratios, the number of DOFs in a conventional ICE powertrain is zero. A parallel HEV has one node combining three mechanical energy flows and thus one DOF. A series hybrid has one node combining three electric energy flows, not considering the electric auxiliaries. Moreover, since the engine output power P_E is not directly linked to the power demand P_D, either the engine speed or the engine torque can be chosen arbitrarily, but not the engine power. Combining this choice with the one power DOF, the number of DOFs can be described as one and one-half. A combined hybrid has in principle two independent nodes and thus two full DOFs. If a planetary gear set or a similar arrangement physically links the two mechanical nodes, the number of DOFs is reduced to one and one-half [4].

The energy-management controller must provide a control vector $u(t)$ whose dimension equals the number of DOFs available in the energy-flow diagram. In a parallel HEV, for instance, the control input is scalar, while the constraint $P_M(t) + P_C(t) = P_D(t)$ linking the motor output power, the engine output power, and the power demand, respectively, must be satisfied at all times. A convenient way to represent $u(t)$ is as a power-split ratio, for instance, as $u(t) = P_M(t)/P_D(t)$ [5], [6].

Various state variables can be identified in a hybrid powertrain. The dimension of the state vector depends on the required level of accuracy. If fuel consumption is the main issue, the system is usually treated as quasistationary, where the inputs of the subsystems are related to the outputs by means of static relationships. Therefore, the only state variable required is the battery charge [6]–[17]. Additional state variables are needed if more energy reservoirs such as super capacitors are present, or if substantial elevation changes, which affect the potential energy of the HEV, are to be included in the optimization.

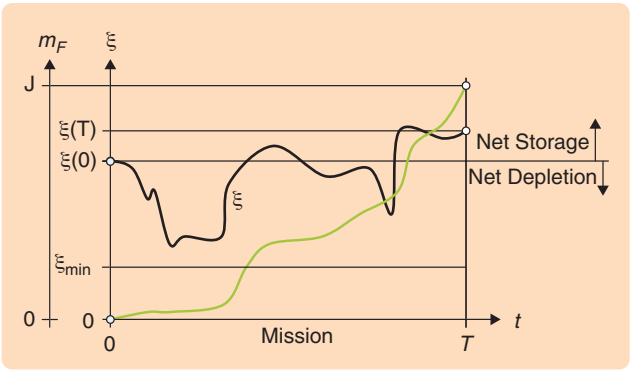

FIGURE 4 Typical trajectories of the state variable $\xi(t)$ and consumed fuel mass $m_F(t)$ along a mission. The consumed fuel mass (grey curve) is delivered by a non-rechargeable energy-storage system and thus cannot decrease. The nondimensional state variable (black curve) is the battery SoC (3), which may have substantial excursions during the mission. The final performance along the mission is represented by the total fuel consumption $J = m_F(T)$ and by the deviation of the SoC $\xi(T)$ from its nominal value $\xi(0)$.

Dynamic models can describe vehicle performance in detail, including the behavior of the driver, the tire/road interaction, and other dynamic effects. These models require the vehicle speed as an additional state [18], [19]. Additional state variables represent the dynamic behavior of the electric motor and the ICE [20]. All of these dynamic effects are faster than the dynamics of the main energy flows in an HEV and, therefore, are not relevant for the problem class considered here.

Numerous disturbance signals affect the system, depending on traffic conditions and driver behavior. These signals, which are denoted by $z(t)$ in this article, comprise among others the road slope and gear ratio in the case of a manual gearbox. The primary system outputs are the fuel-consumption rate, speed, and acceleration of the vehicle.

OPTIMAL BEHAVIOR

The main objective of the energy-management controller is to minimize fuel consumption along a route. Obviously, it is not necessary to minimize the fuel mass-flow rate at each instant of time, but rather the total fuel consumed during a driving mission.

Possible missions are single or multiple repetitions of the governmental test-drive cycles, such as federal urban drive schedule (FUDS) in the United States and MVEG-95 in Europe [21]. Alternatively, missions can be driving patterns recorded on typical routes. During operation, an HEV energy-management controller can explicitly use all of the available information about the mission. The mission information is either provided by the driver or identified implicitly by the control algorithm.

The energy-management controller must respect various hard and soft constraints. For instance, the battery must never be depleted below a specified threshold, while the torque provided by the engine is limited.

Performance Index

As illustrated in Figure 4, the simplest performance index $J = m_F(T)$ is the fuel mass m_F consumed over a mission of duration T. Hence, J can be written as [7]–[10], [13]–[15], [20], [22], [23]

$$J = \int_0^T \dot{m}_F(t, u(t))\, dt. \tag{1}$$

Pollutant emissions can also be included in the performance index J by considering the more general expression

$$J = \int_0^T L(t, u(t))\, dt, \tag{2}$$

where $L(\cdot)$ is the cost function. The emission rates of the regulated pollutants can be included in the performance index (1) by introducing a weighting factor for each pollutant species [5], [16]–[19]. However, if the ICE is a spark-ignited engine operated with stoichiometric air/fuel ratios, its pollutant emissions can usually be reduced to negligible levels

The achievable improvement in fuel economy depends strongly on the vehicle and the driving cycle.

using a three-way catalytic converter. Accordingly, we do not consider pollutant emission as part of the optimization problem, although in practice duty-cycle (on/off operation) or engine shutoff at idle are not acceptable due to excessive pollutant emissions caused by engine or catalyst cooling.

Drivability issues are sometimes included in the optimality criterion. For example, the cost function in [12] includes an antijerk term, which consists of the engine acceleration squared, multiplied by an arbitrary weighting factor. Smoothness and driver-acceptance considerations are included in [15] among the local constraints discussed in the following.

Integral Constraints

Obviously, the drive mode that minimizes the performance index (1) corresponds to a purely electrical strategy in which all of the traction power is provided by the battery. However, if the energy recovered by regenerative braking is not sufficient to sustain the battery charge, this choice can leave the battery completely discharged at the end of the mission.

The state of charge (SoC) of the battery is characterized by the nondimensional scalar

$$\xi(t) \triangleq \frac{Q(t)}{Q_{\max}} = \frac{1}{Q_{\max}} \int_0^t I(\tau)\, d\tau, \tag{3}$$

where $I(t)$ is the battery current, $Q(t)$ is the battery charge at time t, and $Q_{\max}$ is the maximum charge capacity of the battery. Note that the maximum energy stored in the battery is $Q_{\max}V_b$, where V_b is the battery open-circuit voltage.

The sustenance of the energy-storage system is required for the vehicle certification process. Since only small deviations from the nominal value of the SoC are permitted at the end of tests to assess vehicle energy consumption, energy-management controllers must ensure small SoC variations over drive cycles.

In principle, the sustenance constraint can be taken into account in two different ways, namely, as a soft constraint, that is, by penalizing deviations from the initial value of the energy stored at the end of the mission, or as a hard constraint, by requiring that the energy stored at the end of the mission equal the value at the start of the mission.

To represent constraints on the final SoC $\xi(T)$, we add a penalty function $\phi(\xi(T))$ to the performance index (2) to obtain a charge-sustaining performance index of the form

$$J = \phi(\xi(T)) + \int_0^T L(t, u(t))dt. \tag{4}$$

A hard constraint, in which $\xi(T)$ must exactly match the initial value $\xi(0)$, is often explicitly assumed [7]–[10], [13]–[15], [22], [23].

A soft constraint can be represented by a function of the difference $\xi(T) - \xi(0)$. In [18], the quadratic penalty function $\phi(\xi(T)) = \alpha\,(\xi(T) - \xi(0))^2$ is used, where α is a positive weighting factor. In [19], the term $\alpha(\xi(t) - \xi(0))^2$ is included in the cost function.

A quadratic penalty function tends to penalize deviations from the target SoC, regardless of the sign of the deviation. In contrast, a linear penalty function of the type

$$\phi(\xi(T)) = w(\xi(0) - \xi(T)), \tag{5}$$

where w is a positive constant, penalizes battery use, while favoring the energy stored in the battery as a means for saving fuel in the future. Since the penalty function (5) can be expressed as

$$\phi(\xi(T)) = w \int_0^T \dot{\xi}\, dt, \tag{6}$$

the variable $w\dot{\xi}(t)$ can be added to the cost function of (4) to yield the performance index

$$J = \int_0^T (L(t, u(t)) + w\dot{\xi}(t))dt. \tag{7}$$

The parameter w is often chosen arbitrarily [5], [12], [20], while in the regulatory standard SAE J1711 [24], $w = 38$ kWh per gallon of gasoline. Other physically meaningful definitions of w are discussed in the following.

The piecewise-linear penalty function

$$\phi(\xi(T)) = \begin{cases} w_{\text{dis}}(\xi(0) - \xi(T)), & \xi(T) > \xi(0), \\ w_{\text{chg}}(\xi(0) - \xi(T)), & \xi(T) < \xi(0) \end{cases} \tag{8}$$

is at the core of equivalent-consumption minimization strategies (ECMS) [25], which represent real-time implementations of optimal control algorithms. Their formulation is presented in the next section.

Local Constraints

Local constraints can also be imposed on the state and control variables. These constraints mostly concern physical operation limits, notably the maximum engine torque and speed, the motor power, or the battery SoC. Constraints on the control variables are imposed in [15] to enhance smoothness and driver acceptance.

The main limitation of heuristic control concepts is that the various parameters depend strongly on the particular HEV system as well as on the driving conditions.

OPTIMIZATION METHODS

This section presents various approaches to evaluating optimal control laws. These approaches are grouped into three subclasses, namely, static optimization methods, numerical dynamic optimization methods, and closed-form dynamic optimization methods. The third column of Table 1 classifies publications in terms of these techniques.

Static Optimization

Since a mission usually lasts hundreds to thousands of seconds, while, at each time t, multiple values of $u(t)$ must be evaluated, finding the optimal control law by inspecting all possible solutions requires excessive computational and memory resources. The simplified approach described in [8] for a series HEV can easily be extended to parallel HEVs. The relevant controller structure is such that the generator output power $P_G(t)$ is an affine function of the power demand $P_D(t)$, that is,

$$P_G(t) = P_{sa} + \alpha(P_D(t) - P_{da}), \tag{9}$$

where P_{da} is the average value of the power demand, while α and P_{sa} are controller parameters to be optimized. The approach of [8] does not require detailed knowledge of the actual power demand $P_D(t)$, but only of the average value $P_{da} = (1/T)\int_0^T P_D(t)dt$ and its root mean square value

$$R_{eq} = \sqrt{\frac{1}{T}\int_0^T (P_D(t) - P_{da})^2 dt}.$$

The charge sustenance is guaranteed only when duty-cycle operations are performed. For continuous operation of the primary energy source, charge sustenance must be achieved using an additional slow, integrative controller, which makes the controller inherently suboptimal. Dynamic optimization techniques, as presented in the next section, avoid this drawback.

Numerical Optimization Methods

Dynamic programming is commonly used for optimization over a given time period [9], [12], [18], [19], [26]. This method can be used to minimize the performance index (1) in the presence of a hard or a soft constraint on the terminal value of the SoC.

Dynamic programming requires gridding of the state and time variables, and thus the optimal trajectory is calculated only for discretized values of time and SoC. Consequently, the integral (4) and the state dynamics

$$\dot{\xi}(t) = f(t, \xi(t), u(t)) \tag{10}$$

TABLE 1 Some of the research groups currently active in HEV energy control. This classification is based on the optimization method, the real-time implementation, and the experimental/simulation validation.

Ref.	Research Group	Optimization Method	Real-time Implementation	Validation	Other Refs.
[5]	Seoul National University	ECMS	Pattern Recognition	simulation	[43]
[6]	ETH Zurich	ECMS	T-ECMS	experimental	[46]–[48]
[7]	University of Valenciennes	JHB	–	experimental	[25], [35]
[8]	University of Pisa	Static	Continuous Filtering	experimental	[36]
[9]	Ohio State University	ECMS	A-ECMS	experimental	[37], [38]
[10]	Kepler University Linz	LP	–	simulation	[39], [40]
[12]	Tsinghua University	DP	Feedback Control	simulation	[49]
[13]	TU Eindhoven	QP, ECMS	MPC	hardware-in-the-loop	[44]
[14]	Stanford University	LP	–	simulation	
[15]	Hyundai Motor Co.	?	Feedback Control	experimental	
[16]	Ricardo	ECMS	–	experimental	
[17]	Nat. Renewable Energy Lab.	ECMS	Local Conditions	simulation	[32]
[19]	University of Michigan	DP	Feedback Control	simulation	[18]
[20]	Texas A&M University	ECMS	$s = 1$	simulation	[33]
[22]	TU Munich	HJB, ECMS	Heuristic Adaptation	simulation	[34]
[23]	University of Purdue	DP, QP	–	simulation	[41], [42]
[26]	TU Karlsruhe, DaimlerChrysler	DC	MPC	experimental	[45]

are replaced by discrete counterparts. A useful property of all dynamic programming algorithms is that their computational burden increases linearly with the final time T. Since the computational burden increases exponentially with the number of state variables, however, reasonably long missions can be analyzed only if the number of state variables is small. Conveniently, (10) is a scalar equation.

The cost-to-go function $\Gamma(t, \xi)$ is the cost over the optimal trajectory passing through the point (t, ξ) in the time-state space, up to the terminal time T; see Figure 5. With this definition, it follows that $J = \Gamma(0, \xi(0))$. To evaluate $\Gamma(t, \xi)$, the computation proceeds with a time-discretization step Δt backward from time $T - \Delta T$ to time $t = 0$ [27], [28]. The cost-to-go function is then evaluated from the recursion

$$\Gamma(t, \xi(t)) = \min_u \{\Gamma(t + \Delta t, \xi(t) + \dot{\xi}(t, \xi(t), u(t))\Delta t) + L(t, u(t))\Delta t\}. \quad (11)$$

The initial condition for (11) is imposed at time T by

$$\Gamma(T, \xi(T)) = \phi(\xi(T)). \quad (12)$$

The feedback function

$$U(t, \xi(t)) = \arg\min_u \{\Gamma(t + \Delta t, \xi(t) + \dot{\xi}(t, \xi(t), u(t))\Delta t) + L(t, u(t))\Delta t\} \quad (13)$$

represents the control strategy to be stored for real-time operation.

Due to discretization of the state, the values of ξ are either interpolated or approximated by the nearest available values on the grid. In the latter case, rounding can artificially increase or decrease the battery energy calculated over the optimal trajectory. The energy artificially introduced or deleted by rounding determines whether the adopted state-space discretization is acceptable or the number of grid points must be increased.

Improved algorithms with reduced computational time are available. For example, the iterative dynamic programming algorithm in [26] is based on adaptation of the state space. At each iteration, the state space is selected as a small fraction of the entire space, centered around the optimal trajectory evaluated in the previous iteration. Another approach, used by [23], reduces the computing time by splitting the mission into a series of time sections and solving an optimization problem for each of those sections. This approach generally produces a suboptimal solution.

Approximations of the original optimization problem can substantially reduce the computational burden. For instance, if the cost function is linearized with respect to the control variable, a standard linear programming method, such as the simplex algorithm, can be used [10], [14]. Alternatively, quadratic programming [13], [23] requires a quadratic cost function with linear constraints. Of course, all of these simplifications yield suboptimal solutions.

Analytical Optimization Methods

Direct numerical optimization methods require substantial amounts of computational time. One approach that often permits a reduction of the computational effort is based on the minimum principle [7], [10], [22]. This method introduces a Hamiltonian function to be minimized at each time, that is,

$$u(t) = \arg\min_v \{H(t, v, \lambda(t))\}, \quad (14)$$

where

$$H(t, \xi, u, \lambda) \triangleq L(t, u) + \lambda f(t, \xi, u). \quad (15)$$

In this formulation, t is a continuous variable, and the dynamics of the SoC are given by (10). The parameter $\lambda(t)$, which corresponds to the adjoint state in classical optimal control theory, is described by the Euler-Lagrange equation

$$\dot{\lambda}(t) = -\frac{\partial}{\partial \xi} f(t, \xi(t), u(t)). \quad (16)$$

The approximation

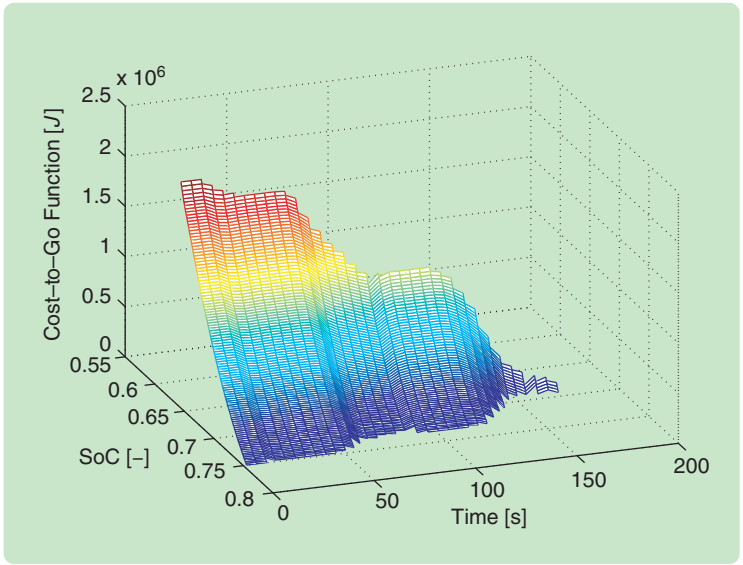

FIGURE 5 Illustrative cost-to-go function Γ given by (11). The data are calculated for the operation of an A-class HEV in the ECE cycle, for a terminal time of 196 s, a target terminal SoC of 0.7, a time step of 1 s, and an SoC discretization of 0.01% of full charge. The target terminal SoC can be reached starting from an initial SoC lower than 0.753 and greater than 0.648.

Approximations of the original optimization problem can substantially reduce the computational burden.

$$\dot{\xi}(t) \approx \tilde{f}(t, u(t)) \tag{17}$$

of (10) is introduced in [7], [10], where the influence of the SoC $\xi(t)$ on the internal battery parameters, such as open-circuit voltage and internal resistance, is neglected. Consequently, (16) becomes $\dot{\lambda} \approx 0$. This assumption may be not valid in other types of HEVs [29], but it is reasonable for hybrid electric HEVs, where only large deviations of the SoC can cause substantial variations of the internal battery parameters. With this assumption, the adjoint state $\lambda(t)$ remains approximately constant along the optimal trajectory. The optimization problem is thus reduced to searching for a constant parameter λ_0 that approximates $\lambda(t)$ for a given mission.

This optimization problem is straightforward: for every time t the Hamiltonian must be minimized with respect to the control variable $u(t)$. Further simplification is possible when the Hamiltonian can be expressed as an explicit function of the control variable. This approach requires an explicit description of $L(t, u(t))$ and the SoC deviation rate $\dot{\xi}(t)$, which can be obtained using simple but accurate modeling tools [30].

In some special applications, the Hamiltonian turns out to be an affine function of the control variable [31]. In this case, the minimum principle states that the optimal control variable is found at its extreme values, depending on the sign of the switching function $\partial H/\partial u$. When the switching function is zero, determining the optimal trajectory requires additional information, typically the second derivative of the Hamiltonian with respect to u.

Equivalent-Consumption Minimization Strategies

The value of the adjoint state $\lambda(t)$ depends primarily on the choice of $\phi(\xi(T))$. In the case of a hard constraint, λ_0 guarantees the fulfillment of the constraint. This value must be determined iteratively, using numerical methods.

In the case of a linear soft constraint such as (5), the value of λ_0 is [7]

$$\lambda_0 = \frac{\partial \phi}{\partial \xi(t)} = -w. \tag{18}$$

If the soft constraint on the final SoC is of the piecewise-linear type (8), then the value of the constant adjoint state must be consistent with the final sign of the SoC deviation [6], in particular,

$$\lambda_0 = \frac{\partial \phi}{\partial \xi(t)} = \begin{cases} -w_{\text{dis}}, & \xi(t) > \xi(0), \\ -w_{\text{chg}}, & \xi(t) < \xi(0). \end{cases} \tag{19}$$

A meaningful expression for the ECMS is obtained when both terms in (15) are reduced to power terms, namely,

$$H(t, s(t), u(t)) = P_F(t, u(t)) + s(t) P_Q(t, u(t)), \tag{20}$$

where $P_F(t, u(t)) = H_{\text{LHV}} \dot{m}_F(t, u(t))$ is the fuel power (H_{LHV} is the lower heating value of the fuel), $P_Q(t, u(t)) = -\dot{\xi}(t, u(t)) V_b Q_{\max}$ is the battery power, and the equivalence factor is

$$s(t) = -\lambda(t) \frac{H_{LHV}}{V_b Q_{\max}}, \tag{21}$$

which represents a nondimensional scaling of the adjoint state. The equivalence factor thus converts battery power to an equivalent fuel power that must be added to the actual fuel power to attain a charge-sustaining control strategy [6], [9]. The ECMS approach is also referred to as a cost-based strategy [16], real-time control strategy [17], or online optimization strategy [22].

Alternative definitions of Hamiltonian-like functions, often derived on a purely heuristic basis, can be reduced to (20). In [22], the Hamiltonian to be minimized is

$$H(t, u(t), \alpha(t)) = P_{\text{diss}}(t, u(t)) + \alpha(t) P_Q(t, u(t)) + K_{\text{cond}}. \tag{22}$$

Similar to (14), the main idea of (22) is to minimize the overall power dissipation $P_{diss}(t, u(t)) = P_F(t, u(t)) + P_Q(t, u(t)) - P_D(t)$. This minimization does not guarantee SoC sustenance. Therefore, the weighted correction $\alpha(t) P_Q(t, u(t))$ is appended to the cost function to penalize the SoC deviations. Moreover, a constant K_{cond} is added to prevent frequent on/off switching of the engine, which leads to additional energy losses and engine wear. Obviously $P_D(t)$ does not depend on $u(t)$ and, therefore, the Hamiltonian function (22) is equivalent to (20) except for K_{cond}.

The nondimensional performance measure of [5] is heuristically designed to locally minimize the fuel-consumption rate and maximize the efficiency of the electrical path. Thus this approach cannot be reduced to a form similar to (20).

In ECMS, the optimization problem is shifted to the evaluation of the equivalence factor $s(t)$. The simplest approach is to assume that a constant value of s is approximately valid for every type of driving condition. In [20], such a value is implicitly assumed to be equal to unity, since the Hamiltonian is simply the sum of the fuel power

The simplest approach is to assume that a constant value of equivalence factor is approximately valid for every type of driving condition.

and battery power. In [16], the objective function is not explicitly shown, but is assumed to be a combination of higher order polynomials based on fuel-conversion efficiency and battery SoC. In general, the equivalence factor s depends on the driving conditions along the mission.

REAL-TIME IMPLEMENTATION

All of the optimization techniques discussed above require knowledge about future driving conditions. This fact makes their implementation in real-time controllers a challenging task. In this section we discuss the level of information required by various control strategies and how such information can be achieved during real-time operation. The fourth column of Table 1 lists the approaches used by the corresponding publications.

Predictive Control

The highest level of information is available when the complete mission is known at the outset. When this is the case, an optimization procedure, such as dynamic programming, can be applied. For public transportation vehicles along fixed routes, where the mission is known in advance, such an approach may be viable. The resulting feedback function $U(t, \xi(t))$ given by (13) can then be implemented in the powertrain control systems.

For passenger cars, the mission is usually unknown at the outset, and the estimation of future driving conditions must be made online. The combination of such an estimation with the application of dynamic programming follows the model-predictive control (MPC) paradigm [13], [26], which requires estimation of the disturbance vector $z(t)$ on a prediction horizon of duration T. Dynamic programming is then used to calculate the optimal control law, which is applied for a shorter control horizon $T_c < T$. In [26], the disturbance vector $z(t)$ is estimated using speed limit, curve radius, and road slope as a function of the distance along the route. These data are obtained by combining onboard and GPS navigation. The vehicle speed is calculated using a dynamic model of the vehicle as a function of the target speed, which is constrained by the speed limit, maximum safe speed especially on curves, and maximum speed allowed by traffic conditions (a parameter that may be available in future applications using radar sensors).

Prediction of the Adjoint State

In strategies derived from optimal control theory, such as ECMS, uncertainty about future driving conditions is transferred to uncertainty on the correct (optimal) value of the constant adjoint state approximation λ_0. The advantage with respect to predictive control is that only one parameter must be determined instead of a disturbance $z(t)$ vector as a function of time. Various methods are available for online estimation of λ_0. These methods, which are described below, can be classified into three approaches depending on the information used, namely, past driving conditions, past and present driving conditions, and past, present, and future driving conditions.

Past Driving Conditions

One technique for estimating λ_0 is based on ideas borrowed from pattern recognition [5]. Optimal values of λ_0 are pre-calculated offline for a set of representative driving patterns, which are composed of urban, expressway, and suburban driving patterns. Up to 24 characteristic parameters, such as average velocity, standstill time, and total time, can be chosen to characterize driving patterns. During real-time operation, a neural network periodically decides which representative driving pattern is closest to the current driving pattern. Then, the energy-management controller switches to the corresponding value of λ_0.

Past and Present Driving Conditions

Pattern recognition methods use information only about past driving conditions. Alternative controllers evaluate λ_0 continuously by adapting λ_0 to the current driving conditions [13], [17], [32] or simply to the current value of the SoC [22].

In some implementations, the equivalence factor $s_0(t)$ is calculated as the partial derivative of the present fuel power with respect to the battery power, that is,

$$s_0(t) = -\frac{\partial P_F}{\partial P_Q}(t). \tag{23}$$

In other words, by varying the control variable $u(t)$, it is possible to obtain a function $P_F(t) = \varphi(P_Q(t))$ that is specific to the current driving conditions. The function $\varphi(\cdot)$, which has a negative slope, is a measure of the fuel cost of the replacement battery energy, which is the battery energy required in the future to compensate current use at the rate $P_Q(t)$.

Consequently, the fuel equivalent of $P_Q(t)$ is simply $\varphi(-P_Q(t))$, while the corresponding Hamiltonian is

In strategies derived from optimal control theory, uncertainty about future driving conditions is transferred to uncertainty on the correct (optimal) value of the constant adjoint state approximation.

$$H(P_F(t), P_Q(t)) = P_F(t) + \varphi(-P_Q(t)), \tag{24}$$

which is consistent with the definition (23).

Such an approach assumes that similar operating conditions will exist in the future, that is, the replacement energy will cost the same amount of fuel energy as it does in the current driving conditions. In general, this assumption leads to trajectories that are neither fuel optimal nor charge sustaining. For this reason, [17] includes an SoC-control factor to their cost function. A modified adaptive strategy of the same type [32] assumes instead that the missing battery energy will be replaced when the ICE operates under more favorable conditions.

The strategy described in [22] mainly emphasizes the SoC-control factor. The weighting factor $\alpha(t)$ of (22), which plays the role of an equivalence factor, is chosen to be an affine function of the current SoC, that is,

$$\alpha(t) = \alpha_0 - \beta(\xi(t) - \xi(0)), \tag{25}$$

where α_0 and β are constants. In other words, when the battery is depleted, the value of α increases so that the use of fuel is favored. Some rules of thumb are given to assign proper values to the parameters α_0 and β. The former, in particular, is calculated using energy considerations that are similar to those underlying (23).

Past, Present, and Future Driving Conditions

Information about the present cannot guarantee optimality of the control action, while the charge cannot be sustained with such an approach. Therefore, future driving conditions must be predicted or estimated, although the disturbance profile $z(t)$ cannot be estimated in detail. In particular, ECMS-based strategies such as telemetry ECMS (T-ECMS) [6] or adaptive ECMS (A-ECMS) [9] do not consider the complete future disturbance vector $z(t)$ along the mission but rather a few characteristic parameters to estimate the optimal value of λ_0. These two approaches are presented in the following.

A piece of information that is usually assumed to be available is the GPS-derived altitude profile of the route that the vehicle intends to follow. The altitude profile provides the road slope as a function of the distance covered. To transform the altitude profile into a slope function of time, the future vehicle speed profile must be estimated. Information on speed limits, which is often considered to be available, can be used for estimation. With regard to traffic conditions, future cars are expected to include radar and other sensors that can be used to obtain this information [6].

The T-ECMS controller is based on (19). Assuming a piecewise-linear soft constraint for the final SoC, the value of the optimal adjoint state depends on the final sign of the SoC deviation. In real-time conditions, this sign is not known. Therefore, the equivalence factor $s(t)$ varies in time between two limit values, namely, s_{chg} and s_{dis}, according to a probability factor $p(t)$, that is,

$$s(t) = p(t)s_{\text{dis}} + (1 - p(t))s_{\text{chg}}. \tag{26}$$

A first-principles analysis shows [47] that $p(t)$ can be calculated as

$$p(t) = \frac{s_{\text{dis}}}{s_{\text{dis}} + s_{\text{chg}}} + \frac{E_e(t) - \Lambda(\bar{E}_m - E_m(t))}{\bar{E}_m - E_m(t)} \frac{\sqrt{s_{\text{dis}} s_{\text{chg}}}}{s_{\text{dis}} + s_{\text{chg}}}, \tag{27}$$

where $E_e(t)$ is the total battery energy used since the start of the mission, $E_m(t)$ is the mechanical energy delivered to the wheels, and $\bar{E}_m$ is a design parameter that defines the extent of the current mission by specifying its total mechanical energy. Therefore, the difference $\bar{E}_m - E_m(t)$ is a measure of the time elapsed in the mission. In (27), a fundamental role is played by the parameter Λ, which is the ratio between the electrical energy that can be recovered and the mechanical energy delivered to the wheels. The parameter Λ is estimated by T-ECMS from energy considerations combined with an estimated future speed profile. This profile, which is a combination of optimal vehicle-trajectory paths, is based on GPS and radar telemetry information. As soon as a new piece of information is obtained from the telemetry system (for instance, the detection of a leading vehicle on the route), a new estimate of the future mission speed profile is obtained. The updated estimate of Λ is used to modify the equivalence factor $s(t)$ in (26) following the rule (27).

The A-ECMS controller [9] also uses a varying equivalence factor $s(t)$, which is adapted in real time to the driving conditions. This algorithm identifies the driving profile of the vehicle and determines the corresponding optimal equivalence factor. The current driving profile is identified by combining past and predicted vehicle-speed data.

Estimation of a synthetic parameter rather than of a detailed picture of future driving conditions also underlies the strategy derived for series HEVs in [8]. The features of the future mission are lumped into an equivalent ripple parameter, defined as the root mean square of the demanded power. An online estimate of this parameter is derived by continuously filtering $P_D(t)$.

Time-Invariant Feedback Controllers

While the optimal and suboptimal strategies described above require global or local estimates, a simpler approach consists of storing the control algorithm in the form of a lookup table, providing the control variable $u(t)$ as a function of the current driving conditions and state variables. Generally, the feedback quantities that parameterize the control variable are the vehicle speed, power demand $P_D(t)$, and battery SoC. In place of vehicle speed, the wheel or engine speed is often used. Likewise, in place of power demand, it is possible to use the torque demand or vehicle acceleration, in the latter case neglecting the influence of road slope.

Many existing energy-management strategies employ heuristic control techniques. Heuristic rules are often used based on thresholds of the feedback quantities [3]. Consequently, the control variable $u(t)$ typically assumes integer values, 0 for engine only and 1 for motor only, unless the torque constraints are active. Alternatively, the use of fuzzy logic is investigated in [11]. In this case, the typical outputs of the feedback control law are not discrete values for $u(t)$ but rather are fuzzy values such as high engine use or low motor use.

A substantial improvement can be obtained using dynamic optimization to build a feedback map [12], [15], [18]. The optimal solution found with dynamic programming is statistically analyzed in terms of input and state variables, from which implementable rules are extracted to construct the control strategy. To limit the complexity of the feedback map, only two input variables are usually allowed. Examples include torque demand and SoC [18], power demand and SoC [12], and wheel speed and power demand [15]. Although this approach performs well in real hybrid vehicles, it is based on optimization with respect to a specific drive cycle and, in general, it is neither optimal nor charge-sustaining for other cycles. Moreover, the feedback solution obtained using dynamic programming cannot be implemented directly, and the rule-extraction process is not straightforward.

To overcome these drawbacks, the procedure of [18] is extended in [19] using stochastic dynamic programming. To obtain a time-invariant control strategy, an infinite-horizon optimization problem is solved. The feedback control law derived with stochastic dynamic programming is applicable to general driving conditions. Its validity is tested in [19] over regulatory as well as random drive cycles.

CONCLUSIONS

Global optimization techniques, such as dynamic programming, serve mainly to evaluate the potential fuel economy of a given powertrain configuration. Unless the future driving conditions can be predicted during real-time operation, these control laws cannot be implemented directly, but the results obtained using this noncausal approach establish a benchmark for evaluating the optimality of realizable control strategies.

Real-time controllers must be simple in order to be implementable with limited computation and memory resources. Moreover, manual tuning of control parameters should be avoided. In principle, the realization of a real-time controller can be accomplished in several ways. This article has analyzed two approaches, namely, feedback controllers and ECMS. Both of these approaches can lead to system behavior that is close to optimal, with feedback controllers based on dynamic programming. Since the computational burden of both approaches is not too intensive, existing hardware technology is sufficient for most typical applications.

To guarantee behavior that is sufficiently close to optimal, a real-time controller must adapt itself to varying driving conditions. Feedback controllers are based on static maps and thus do not offer this functionality. A possible approach to extending their validity is to design them based on stochastic dynamic programming. In contrast, ECMS controllers are based on a few key control parameters (usually, the equivalence factor between electricity and fuel) that can be adapted during real-time operation. Relevant approaches include the use of GPS systems and radar telemetry.

How the necessary information about the future driving conditions can be obtained remains an open question. Additional challenges stem from the need to apply optimal energy-management controllers to advanced HEV architectures, such as combined and plug-in HEVs, as well as to optimization problems that include performance indices in addition to fuel economy, such as pollutant emissions, driveability, and thermal comfort.

REFERENCES

[1] F. Porsche, *The First Hybrid Vehicle* [Online]. Available: http://www.hybrid-vehicle.org

[2] L. Guzzella and A. Sciarretta, *Vehicle Propulsion Systems. Introduction to Modeling and Optimization*. Berlin: Springer-Verlag, 2005, p. 190.

[3] *A Guide to Hybrid Synergy Drive*, Toyota Motor Corp. [Online]. Available: the URL http://www.toyota.co.jp

[4] L. Guzzella and A. Sciarretta, *Vehicle Propulsion Systems. Introduction to Modeling and Optimization*. Berlin: Springer-Verlag, 2005, p. 67.

[5] S. Jeon, S. Jo, Y. Park, and J. Lee, "Multi-mode driving control of a parallel hybrid electric vehicle using driving pattern recognition," *ASME J. Dynamic Syst., Meas., Control*, vol. 124, pp. 141–149, 2002.

[6] A. Sciarretta, L. Guzzella, and M. Back, "A real-time optimal control strategy for parallel hybrid vehicles with on-board estimation of control parameters," in *Proc. IFAC Symp. Advances Automotive Control*, Salerno, Italy, 2004, Paper 136, pp. 502–507.

[7] S. Delprat, J. Lauber, T.M. Guerra, and J. Rimaux, "Control of a parallel hybrid powertrain: optimal control," *IEEE Trans. Veh. Technol.*, vol. 53, no. 3, pp. 872–881, 2004.

[8] S. Barsali, C. Miulli, and A. Possenti, "A control strategy to minimize fuel consumption of series hybrid electric vehicles," *IEEE Trans. Energy Conversion*, vol. 19, no. 1, pp. 187–195, 2004.
[9] C. Musardo, G. Rizzoni, and B. Staccia, "A-ECMS: an adaptive algorithm for hybrid electric vehicle energy management," in *Proc. 44th IEEE Conf. Decision Control, 2005 European Control Conf.*, Seville, Spain, 2005, pp. 1816–1823.
[10] G. Steinmauer and L. del Re, "Optimal control of dual power sources," in *Proc. 2001 IEEE Int. Conf. Control Applications*, Mexico City, Mexico, 2001, pp. 422–442.
[11] M. Salman, N. Schouten, and N. Kheir, "Control strategies for parallel hybrid vehicles," in *Proc. 2000 American Control Conf.*, Chicago, IL, 2000, pp. 524–529.
[12] Y. Zhu, Y. Chen, G. Tian, H. Wu, and Q. Chen, "A four-step method to design an energy management strategy for hybrid vehicles," in *Proc. 2004 American Control Conf.*, Boston, MA, pp. 156–161, 2004.
[13] M. Koot, J. Kessels, B. de Jager, W. Heemels, P. van den Bosch, and M. Steinbuch, "Energy management strategies for vehicular electric power systems," *IEEE Trans. Vehicle Technol.*, vol. 54, no. 3, pp. 1504–1509, 2005.
[14] E.D. Tate and S.P. Boyd, "Finding ultimate limits of performance for hybrid electric vehicles," *Proc. SAE*, Paper 2000-01-3099, 2000.
[15] H. Yoon and S. Lee, "An optimized control strategy for parallel hybrid electric vehicle," *Proc. SAE*, Paper 2003-01-1329, 2003.
[16] L. Buie, M. Fry, P. Fussey, and C. Mitts, "An application of cost based power management control strategies to hybrid fuel cell vehicles," *Proc. SAE*, Paper 2004-01-1299, 2004.
[17] V.H. Johnson, K.B. Wipke, and D.J. Rausen, "HEV control strategy for real-time optimization of fuel economy and emissions," *Proc. SAE*, Paper 2000-01-1543, 2000.
[18] C.-C. Lin, H. Peng, J.W. Grizzle, and J.-M. Kang, "Power management strategy for a parallel hybrid electric truck," *IEEE Trans. Control Syst. Technol.*, vol. 11, no. 6, pp. 839–849, 2003.
[19] C.-C. Lin, H. Peng, and J.W. Grizzle, "A stochastic control strategy for hybrid electric vehicle," in *Proc. 2004 American Control Conf.*, Boston, MA, 2004, pp. 4710–4715.
[20] J.-S. Won, R. Langari, and M. Ehsani, "An energy management and charge sustaining strategy for a parallel hybrid vehicle with CVT," *IEEE Trans. Control Syst. Technol.*, vol. 13, no. 2, pp. 313–320, 2005.
[21] L. Guzzella and A. Sciarretta, *Vehicle Propulsion Systems. Introduction to Modeling and Optimization*. Berlin: Springer-Verlag, 2005, p. 21.
[22] A. Kleimaier and D. Schröder, "An approach for the online optimized control of a hybrid powertrain," in *Proc. 7th Int. Workshop Advanced Motion Control*, Maribor, Slovenia, 2002, pp. 215–220.
[23] R. Zhang and Y. Chen, "Control of hybrid dynamical systems for electric vehicles," in *Proc. American Control Conf.*, Arlington, VA, 2001, pp. 2884–2889.
[24] *Recommended Practice for Measuring the Exhaust Emissions and Fuel Economy of Hybrid-Electric Vehicles*, SAE Standard J1711 [Online]. Available: http://www.sae.org/servlets/productDetail?PROD_TYP=STD&PROD_CD=J1711&HIER_CD=TEVHYB&WIP_S=YES
[25] G. Paganelli, T.-M. Guerra, S. Delprat, J.-J. Santin, M. Delhom, and E. Combes, "Simulation and assessment of power control strategies for a parallel hybrid car," *Proc. IMechE, Part D: J. Auto. Eng.*, vol. 214, no. 7, pp. 705–717, 2000.
[26] M. Back, Prädiktive Antriebsregelung zum energieoptimalen Betrieb von Hybridfahrzeugen, Diss. Univ. Karlsruhe, [Online]. Available: http://www.ubka.uni-karlsruhe.de 2005.
[27] A.E. Bryson and Y.C. Ho, *Applied Optimal Control*. New York: Taylor & Francis, 1975.
[28] D.P. Bertsekas, *Programming and Optimal Control.* Nashua, NH: Athena Scientific, 2000.
[29] Z. Filipi, L. Louca, B. Daran, C.-C. Lin, U. Yildir, B. Wu, M. Kokkolaras, D. Assanis, H. Peng, P. Papalambros, and J. Stein, "Combined optimization of design and power management of the hydraulic hybrid propulsion system for the 6 × 6 medium truck," *Int. J. Heavy Veh. Syst*, vol. 11, no. 3/4, pp. 371–401, 2004.
[30] G. Rizzoni, L. Guzzella, and B. Baumann, "Unified modeling of hybrid electric vehicle drivetrains," *IEEE/ASME Trans. Mechatronics*, vol. 4, no. 3, pp. 246–257, 1999.
[31] A. Sciarretta, L. Guzzella, and J. van Baalen, "Fuel optimal trajectories of a fuel cell vehicle," in *Proc. IFAC Int. Conf. Advances Vehicle Control Safety*, Genoa, Italy, Paper AVCS127, 2004.
[32] B. Jeanneret and T. Markel, "Adaptive energy management strategy for fuel cell hybrid vehicles," *Proc. SAE*, Paper 2004-01-1298, 2004.
[33] J.-S. Won and R. Langari, "Intelligent energy management agent for a parallel hybrid vehicle—Part II: torque distribution, charge sustenance strategies, and performance results," *IEEE Trans. Vehicle Technol.*, vol. 54, no. 3, pp. 935–953, 2005.
[34] A. Kleimaier and D. Schröder, "Optimization strategy for design and control of a hybrid vehicle," in *Proc. 6th Int. Workshop Advanced Motion Control*, Nagoya, Japan, 2000, pp. 459–464.
[35] S. Delprat, T.-M. Guerra, and J. Rimaux, "Control strategy for hybrid vehicles: synthesis and evaluation," in *Proc. 2003 IEEE Vehicle Technol. Conf.*, Orlando, FL, 2003, pp. 3246–3250.
[36] S. Barsali, M. Ceraolo, and A. Possenti, "Techniques to control the electricity generation in a series hybrid electrical vehicle," *IEEE Trans. Energy Conversion*, vol. 17, no. 2, pp. 260–266, 2002.
[37] P. Pisu, K. Koprubasi, and G. Rizzoni, "Energy management and driveability control problems for hybrid electric vehicles," in *Proc. 44th IEEE Conf. Decision Control, 2005 European Control Conf.*, Seville, Spain, 2005, pp. 1824–1830.
[38] P. Pisu and G. Rizzoni, "A supervisory control strategy for series hybrid electric vehicles with two energy storage systems," in *Proc. 2005 IEEE Conf. Vehicle Power Propulsion*, Chicago, IL, 2005, pp. 65–72.
[39] G. Steinmaurer and L. del Re, "Receding horizon suboptimal control for fuel consumption optimization of hybrid vehicles," in *Proc. 2000 Asian Control Conf.*, Shanghai, China, 2000, pp. 1332–1337.
[40] G. Steinmaurer and L. del Re, "Optimal energy management for mild hybrid operation of vehicles with an integrated starter generator," *Proc. SAE*, Paper 2005-01-0280, 2005.
[41] R. Zhang and Y. Chen, "Control of hybrid dynamical systems for electric vehicles," in *Proc. 2001 American Control Conf.*, Arlington, VA, 2001, pp. 2884–2889.
[42] H. Zhang, Y. Zhu, G. Tien, Q. Chen, and Y. Chen, "Optimal energy management strategy for hybrid electric vehicles," *SAE Trans. J. Engines*, vol. V, no. 113-3, pp. 408–417, 2004.
[43] S.I. Jeon, S.T. Jo, H.S. Jo, Y.I. Park, and J.M. Lee, "The development of the simulation program for laying out the hybrid vehicle," in *Proc. 1999 Spring Conf.*, Korea Society Automotive Engineers, Kwang-ju, Korea, 1999, pp. 713–719.
[44] J. Kessels, P. van den Bosch, M. Koot, and B. de Jager, "Energy management for vehicle power net with flexible electric load demand," in *Proc. 2005 IEEE Conf. Control Applications*, Toronto, Canada, 2005, pp. 1504–1509.
[45] M. Back, S. Terwen, and V. Krebs, "Predictive powertrain control for hybrid electric vehicles," in *Proc. IFAC Symp. Advances Automotive Control*, Salerno, Italy, 2004, Paper no. 112, pp. 121–126.
[46] A. Sciarretta, C. Onder, and L. Guzzella, "On the power split control of parallel hybrid vehicles: from global optimization to real-time control," *at–Automatisierungstechnik*, vol. 51, no. 5, pp. 195–203, 2003.
[47] A. Sciarretta, M. Back, and L. Guzzella, "Optimal control of parallel hybrid electric vehicles," *IEEE Trans. Control Syst. Technol.*, vol. 12, no. 3, pp. 352–363, 2004.
[48] R. Cipollone and A. Sciarretta, "Analysis of the potential performance of a combined hybrid vehicle with optimal supervisory control," in *Proc. IEEE Int. Conf. Control Applications*, Munich, Germany, 2006, pp. 2802–2807.
[49] H. Zhang, Y. Zhu, G. Tian, Q. Chen, and Y. Chen, "Optimal Energy Management Strategy for Hybrid Electric Vehicles," *Proc. SAE*, Paper 2004-01-0576, 2004.

AUTHOR INFORMATION

Antonio Sciarretta (antonio.sciarretta@ifp.fr) received the doctorate degree from the University of L'Aquila, Italy. He is currently a research engineer at the Institut Français du Pétrole (IFP) and a lecturer at the ETH Zurich. His research interests are in modeling, optimization, and control of vehicle and engine systems. He can be contacted at IFP, 1-4 av. de Bois Préau, GIR 118, 92852 Rueil-Malmaison, France.

Lino Guzzella received the doctorate degree from ETH Zurich, where he is a professor of thermotronics in the Department of Mechanical and Process Engineering. His research interests are in modeling of dynamic systems, nonlinear and robust control, and applications of these ideas to thermal and automotive systems.